Finite Displacement Analysis Using Rotational Degrees of Freedom about Three Right-angled Axes

Humihiko Gotou [1], Takashi Kuwataka[1], Terumasa Nishihara[1] and Tetsuo Iwakuma[1]

Abstract: The stiffness equation in finite displacement problems is often derived from the virtual work equation, partly in order to avoid the complicated formulation based on the potential functional. Describing the virtual rotational angles by infinitesimal rotational angles about three axes of the right-angled Cartesian coordinate system, we formulate tangent stiffness equations whose rotational degrees of freedom are described by rotational angles about the three axes. The rotational degrees of freedom are useful to treat three rotational components in nodal displacement vectors as vector components for coordinate transformation, when non-vector components like Euler's angles are used to describe finite rotations. In this paper accuracy of the formulations is numerically demonstrated.

keyword: Euler's angles, rotational pseudo-vector, rotational degrees of freedom

1 Introduction

Since finite rotational displacements in space can not be expressed as linearly independent components on linear space, rotational degrees of freedom in finite displacement analysis for spacial beams and plates are often treated as some kinds of three independent parameters, by which a rotation group, that is, a transformation matrix is described. Finite displacement formulations are often derived from the first variation of the total potential energy, that is, the virtual work equation, so that it is not necessary to define the potential functional on the manifold which includes the rotation group. Substitution of strain-displacement relationship into the internal virtual work derives a stiffness equation. In order to express the displacement field, one can use a rotation group (transformation matrix) described by three independent parameters such as: axial-vector compo-

nents (rotational pseudo-vector [Argyris (1982); Kamita and Kondo (1995); Atluri and Cazzani (1995); Ishihara (1996); Okamoto and Omura (2003)], Rodrigues parameters [Argyris (1982); Cheng and Gupta (1989)], Euler's angles [Goto, Li, Kasugai and Obata (1995); Gotou, Kobayasi and Iwakuma (1997); Gotou, Koyabasi, Saiki and Iwakuma (1998); Béda (2003)] or direction cosines expressed as nine dependent components [Goto, Morikawa and Matsuura (1998)]. Any displacement fields expressed by those rotational components more or less make strain-displacement relationship complicated. It is difficult to directly derive the finite element formulation by substitution of the strain-displacement relationship into the internal virtual work. In place of that, it is usual to utilize the linear stiffness equation which holds in the local coordinate system co-rotating with rigid body displacement components of a element. In order to transform the nodal displacement vector of the element described in the local coordinate system into that in the global coordinate system, one can use transformation matrix described by functions of the rotational parameters. On the other hand, one can derive the relationship to transform nodal external force vectors in the local coordinate system into those in the global coordinate system, by equating the external virtual work in the local coordinate system with that in the global coordinate system. Based on such derivation, one can choose infinitesimal rotational angles about three axes of the right-angled Cartesian coordinate system as rotational degrees of freedom, because the virtual displacements are infinitesimal. In this paper we derive one of such formulations, whose rotational degrees of freedom are angles about the three axes and numerically demonstrate the accuracy.

[1] Department of Civil Engineering
Tohoku University, Japan
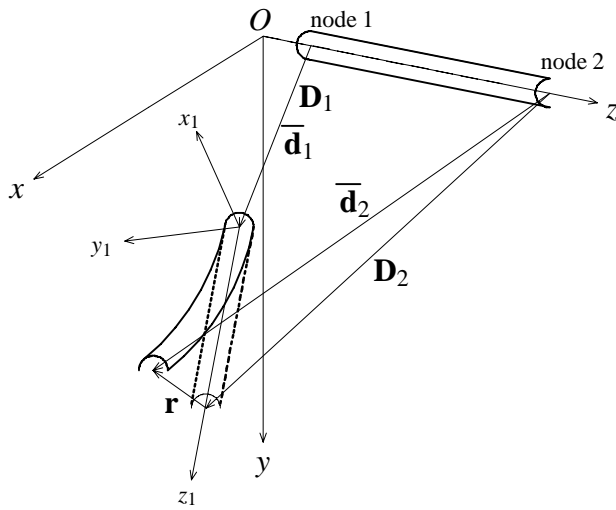
Figure 1 : Nodal displacement vectors

2 Formulation for beam element

2.1 *Nodal relative displacement*

Consider a straight beam element lying along z-axis in a spacially fixed coordinate system (x, y, z) as shown in (Fig. 1). Firstly we denote the nodal displacement vector by

$$
\begin{aligned}
\overline{\mathbf{d}} &\equiv \lfloor \overline{\mathbf{d}}_1^T \ \overline{\mathbf{d}}_2^T \rfloor^T && (1)\\
\overline{\mathbf{d}}_i &\equiv \lfloor u_i \ v_i \ w_i \ \theta_{xi} \ \theta_{yi} \ \theta_{zi} \ \lambda_i \rfloor^T \quad (i=1,2)
\end{aligned}
$$

where u_i, v_i and w_i are translational displacements in the directions of x, y and z-axes respectively; θ_{xi}, θ_{yi} and θ_{zi} are rotational angles in the right-hand-screw directions of x, y and z-axes respectively; and λ_i is $\frac{d\theta_{zi}}{dz}$.

θ_{xi}, θ_{yi} and θ_{zi} in Eq. 1 can not express finite rotations but we use them to define infinitesimal relative rotational angles between two nodes later on.

Secondly we denote the same nodal displacement vector using Euler's angles (α, γ, ϕ) as follows so that they can express finite rotations.

$$
\begin{aligned}
\mathbf{d} &\equiv \lfloor \mathbf{d_1}^T \ \mathbf{d_2}^T \rfloor^T && (2)\\
\mathbf{d_i} &\equiv \lfloor u_i \ v_i \ w_i \ \alpha_i \ \gamma_i \ \phi_i \ \lambda_i \rfloor^T \quad (i=1,2)
\end{aligned}
$$

When an element whose node 1 is located at the point $(0,0,z_0)$ and whose node 2 is located at the point

$(0,0,z_0+\ell)$ moves as a rigid body, the nodal displacement vector of the node 1 is written as follows.

$$
\mathbf{D}_1 \equiv \lfloor u_1 \ v_1 \ w_1 \ \theta_{x1} \ \theta_{y1} \ \theta_{z1} \ 0 \rfloor^T \tag{3}
$$

Using the displacement vector of node 1 $\mathbf{D}_1$ we can write the nodal displacement vector of the node 2 as

$$
\mathbf{D_2} =
\begin{bmatrix}
\left[\left\{ \begin{array}{c} u_1 \\ v_1 \\ w_1 \end{array} \right\} + \mathbf{T} \left\{ \begin{array}{c} 0 \\ 0 \\ \ell \end{array} \right\} - \left\{ \begin{array}{c} 0 \\ 0 \\ \ell \end{array} \right\} \right] \\
\theta_{x1} \\
\theta_{y1} \\
\theta_{z1} \\
0
\end{bmatrix}
\tag{4}
$$

where $\mathbf{T}$ is a transformation matrix which transforms local coordinates (x_ℓ, y_ℓ, z_ℓ) into the global ones (x, y, z) on the spacially fixed coordinate system and is written as follows [Gotou, Kobayasi, Saiki and Iwakuma (1998)].

$$
\mathbf{T}(\alpha, \gamma, \phi) = \tag{5}
$$
$$
\begin{bmatrix}
\cos\phi\cos\gamma & -\sin\phi\cos\gamma & \cos\alpha\sin\gamma \\
-\sin\phi\sin\alpha\sin\gamma & -\cos\phi\sin\alpha\sin\gamma & \\
\sin\phi\cos\alpha & \cos\phi\cos\alpha & \sin\alpha \\
-\cos\phi\sin\gamma & \sin\phi\sin\gamma & \cos\alpha\cos\gamma \\
-\sin\phi\sin\alpha\cos\gamma & -\cos\phi\sin\alpha\cos\gamma &
\end{bmatrix}
$$

Here we name the displacement vector $\mathbf{D}_1$ or $\mathbf{D}_2$ 'rigid body displacement vector' of the each node and write the nodal rigid body displacement vector of one element as follows.

$$
\mathbf{D} \equiv \lfloor \ \mathbf{D_1}^T \ \ \mathbf{D_2}^T \ \rfloor^T \tag{6}
$$

Suppose that the element was deformed and now has displacements expressed by $\overline{\mathbf{d}}$. Here we define local coordinate system (x_1, y_1, z_1), whose origin is located at the node 1 and whose z_1-axis is tangent to the element axis at the node 1 as shown in Fig. (1). We define relative displacement components of $\overline{\mathbf{d}}$ to the rigid body displace-

ment vector $\mathbf{D}$ as follows.

$$\mathbf{r} \equiv \lfloor \mathbf{r}_1^T \; \mathbf{r}_2^T \rfloor^T \tag{7}$$

$$\mathbf{r}_1 \equiv \overline{\mathbf{d}}_1 - \mathbf{D}_1 = \lfloor 0 \; 0 \; 0 \; 0 \; 0 \; 0 \; \lambda_1 \rfloor^T$$

$$\mathbf{r}_2 \equiv \overline{\mathbf{d}}_2 - \mathbf{D}_2$$

$$= \begin{bmatrix} \left\{ \begin{matrix} u_2 - u_1 \\ v_2 - v_1 \\ w_2 - w_1 \end{matrix} \right\} - \mathbf{T} \left\{ \begin{matrix} 0 \\ 0 \\ \ell \end{matrix} \right\} + \left\{ \begin{matrix} 0 \\ 0 \\ \ell \end{matrix} \right\} \\ \theta_{x2} - \theta_{x1} \\ \theta_{y2} - \theta_{y1} \\ \theta_{z2} - \theta_{z1} \\ \lambda_2 \end{bmatrix}$$

In this way the rigid body displacement vector $\mathbf{D}_1$ represents rigid body motion of the element so that the relative displacement vector $\mathbf{r}_2$ represents substantial deformation of the element. Increasing number of element divisions so that $\mathbf{r}_2$ becomes small, we can evaluate the relative displacement within the small displacement theory, if the small strain assumption holds on all deformation paths. As mentioned above, θ_{xi}, θ_{yi} and θ_{zi} can not express finite rotations but their small relative rotations in Eq.7 can be approximately related with the components of Euler's angles by geometrical consideration as follows [Gotou, Kobayasi and Iwakuma (1997); Gotou, Kobayasi, Saiki and Iwakuma (1998)].

$$\left\{ \begin{matrix} \Delta\theta_x \\ \Delta\theta_y \\ \Delta\theta_z \end{matrix} \right\} \simeq \begin{bmatrix} -\cos\gamma & 0 & \sin\gamma\cos\alpha \\ 0 & 1 & \sin\alpha \\ \sin\gamma & 0 & \cos\gamma\cos\alpha \end{bmatrix} \left\{ \begin{matrix} \Delta\alpha \\ \Delta\gamma \\ \Delta\phi \end{matrix} \right\} \tag{8}$$

Replacing infinitesimal angle components in Eq.8 by the relative rotations of the node 2 to the node 1 and replacing the finite Euler's angles in Eq.8 by average rotational angles of the both nodes, the following approximation is derived.

$$\mathbf{r}_2 = \tag{9}$$

$$\begin{bmatrix} u_2 - u_1 - \ell\cos\alpha_1\sin\gamma_1 \\ v_2 - v_1 - \ell\sin\alpha_1 \\ w_2 - w_1 - \ell(\cos\alpha_1\cos\gamma_1 - 1) \\ \begin{bmatrix} -\cos\frac{\gamma_1+\gamma_2}{2} & 0 & \sin\frac{\gamma_1+\gamma_2}{2}\cos\frac{\alpha_1+\alpha_2}{2} \\ 0 & 1 & \sin\frac{\alpha_1+\alpha_2}{2} \\ -\sin\frac{\gamma_1+\gamma_2}{2} & 0 & \cos\frac{\gamma_1+\gamma_2}{2}\cos\frac{\alpha_1+\alpha_2}{2} \end{bmatrix} \left\{ \begin{matrix} \alpha_2-\alpha_1 \\ \gamma_2-\gamma_1 \\ \phi_2-\phi_1 \end{matrix} \right\} \\ \lambda_2 \end{bmatrix}$$

2.2 Stiffness equation

We define the nodal force vector which does work for $\overline{\mathbf{d}}$

by

$$\mathbf{f} \equiv \lfloor \mathbf{f}_1^T \; \mathbf{f}_2^T \rfloor^T \tag{10}$$

$$\mathbf{f_i} \equiv \lfloor F_{xi} \; F_{yi} \; F_{zi} \; M_{xi} \; M_{yi} \; M_{zi} \; M_{\lambda i} \rfloor^T$$
$$(i = 1, 2)$$

where F_{xi}, F_{yi} and F_{zi} are nodal forces in the directions of x, y and z-axes respectively; M_{xi}, M_{yi} and M_{zi} are nodal moments in the right-hand-screw directions of x, y and z-axes respectively; and $M_{\lambda i}$ is nodal bi-moment. Equating the virtual work in the global fixed coordinate system (x, y, z) with those in the local coordinate system (x_1, y_1, z_1) we can write the virtual work equation as [Kamita and Kondo (1995); Goto, Li, Kasugai and Obata (1995); Gotou, Kobayasi, Saiki and Iwakuma (1998)]

$$\mathbf{f}^T \delta\overline{\mathbf{d}} = \mathbf{f}_\ell^T \delta\mathbf{r}_\ell \tag{11}$$

where vectors with a subscript ℓ denote vectors whose components are described in the local coordinate system. Defining the following transformation matrix

$$\mathbf{T}_o \equiv \begin{bmatrix} \mathbf{T}_1 & \mathbf{O}_{77} \\ \mathbf{O}_{77} & \mathbf{T}_1 \end{bmatrix} \tag{12}$$

$$\mathbf{T}_1 \equiv \begin{bmatrix} \mathbf{T} & \mathbf{O}_{33} & \mathbf{O}_{31} \\ \mathbf{O}_{33} & \mathbf{T} & \mathbf{O}_{31} \\ \mathbf{O}_{13} & \mathbf{O}_{13} & 1 \end{bmatrix}$$

where $\mathbf{O}_{ij}$ denotes a $i \times j$ zero matrix, we substitute the relation $\mathbf{r}_\ell = \mathbf{T}_o^T \mathbf{r}$ into Eq.11 and rewrite it as follows

$$\begin{aligned} \mathbf{f}^T \delta\overline{\mathbf{d}} &= \mathbf{f}_\ell^T \delta\{\mathbf{T}_o^T \mathbf{r}\} \\ &= \mathbf{f}_\ell^T \left[\frac{\partial \mathbf{T}_o^T}{\partial \mathbf{d}} \mathbf{r} + \mathbf{T}_o^T \frac{\partial \mathbf{r}}{\partial \mathbf{d}} \right] \delta\mathbf{d} \\ &= \mathbf{f}_\ell^T \mathbf{R} \delta\mathbf{d} \\ &= \mathbf{f}_\ell^T \mathbf{R} \mathbf{E} \delta\overline{\mathbf{d}} \end{aligned} \tag{13}$$

where

$$\mathbf{R} \equiv \left[\frac{\partial \mathbf{T}_o^T}{\partial \mathbf{d}} \mathbf{r} + \mathbf{T}_o^T \frac{\partial \mathbf{r}}{\partial \mathbf{d}} \right] \tag{14}$$

and $\mathbf{E}$ is a matrix derived from the inverse relation of Eq.8 so that $\delta\mathbf{d}$ is equal to $\mathbf{E}\delta\overline{\mathbf{d}}$ as follows

$$\mathbf{E} \equiv \begin{bmatrix} \mathbf{e_1} & \mathbf{O}_{77} \\ \mathbf{O}_{77} & \mathbf{e_2} \end{bmatrix} \tag{15}$$

$$\mathbf{e_i} \equiv \begin{bmatrix} \mathbf{I} & \mathbf{O}_{33} & \mathbf{O}_{31} \\ \mathbf{O}_{33} & \begin{bmatrix} -\cos\gamma & 0 & \sin\gamma \\ -\sin\gamma\tan\alpha & 1 & -\cos\gamma\tan\alpha \\ \sin\gamma/\cos\alpha & 0 & \cos\gamma/\cos\alpha \end{bmatrix} & \mathbf{O}_{31} \\ \mathbf{O}_{13} & \mathbf{O}_{13} & 1 \end{bmatrix}$$
$$(i = 1, 2)$$

where $\mathbf{I}$ denotes a 3×3 identity matrix. If strains are very small during any deformation history, we can relate $\mathbf{f}_\ell$ and $\mathbf{r}_\ell$ by the linear elastic stiffness matrix $\mathbf{K}$ as follows.

$$\mathbf{f}_\ell = \mathbf{K}\mathbf{r}_\ell \tag{16}$$

From Eq.13 and Eq.16, we obtain the following relation.

$$\begin{aligned} \mathbf{f} &= \mathbf{E}^T\mathbf{R}^T\mathbf{f}_\ell \\ &= \mathbf{E}^T\mathbf{R}^T\mathbf{K}\mathbf{T_o}^T\mathbf{r} \end{aligned} \tag{17}$$

In order to solve Eq.17 by Newton-Raphson Method and Arc Length Method we deduce the incremental equation, that is, the tangent stiffness equation as follows.

$$\begin{aligned} \Delta\mathbf{f} &= \frac{\partial}{\partial\mathbf{d}}\left[\mathbf{E}^T\mathbf{R}^T\mathbf{K}\mathbf{T_o}^T\mathbf{r}\right]\Delta\mathbf{d} \\ &= \left[\frac{\partial\mathbf{E}^T}{\partial\mathbf{d}}\mathbf{R}^T\mathbf{K}\mathbf{T_o}^T\mathbf{r}\mathbf{E} + \mathbf{E}^T\left[\frac{\partial\mathbf{R}^T}{\partial\mathbf{d}}\mathbf{K}\mathbf{T_o}^T\mathbf{r} + \mathbf{R}^T\mathbf{K}\mathbf{R}\right]\mathbf{E}\right]\Delta\overline{\mathbf{d}} \\ &\equiv \mathbf{K}_1\Delta\overline{\mathbf{d}} \end{aligned} \tag{18}$$

While we derived the above tangent stiffness equation only for the case in which we used Euler's angles to describe finite rotations, we can also derive it for other rotational parameters like rotational pseudo-vector components and so on in the same manner. When we use Euler's angles, the relation $\mathbf{d} = \mathbf{E}\delta\overline{\mathbf{d}}$ is necessary to make it possible to transform rotational degrees of freedom into the other coordinate system, if we want to analyze curved beams and so on. When we use rotational pseudo-vector components, which can be transformed as 'vector' components, the relation is not always necessary and the tangent stiffness equation can be written as follows.

$$\begin{aligned} \Delta\mathbf{f} &= \frac{\partial}{\partial\mathbf{d}}\left[\mathbf{R}^T\mathbf{K}\mathbf{T_o}^T\mathbf{r}\right]\Delta\mathbf{d} \\ &= \left[\frac{\partial\mathbf{R}^T}{\partial\mathbf{d}}\mathbf{K}\mathbf{T_o}^T\mathbf{r} + \mathbf{R}^T\mathbf{K}\mathbf{R}\right]\Delta\mathbf{d} \\ &\equiv \mathbf{K}_2\Delta\mathbf{d} \end{aligned} \tag{19}$$

However the matrix $\mathbf{R}$ derived for the rotational pseudo-vector becomes much more complicated than $\mathbf{R}$ for
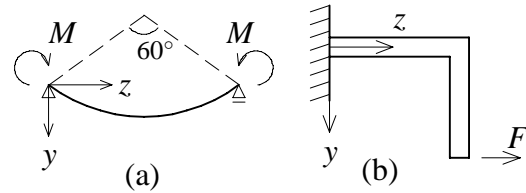
Figure 2 : Analyzed models
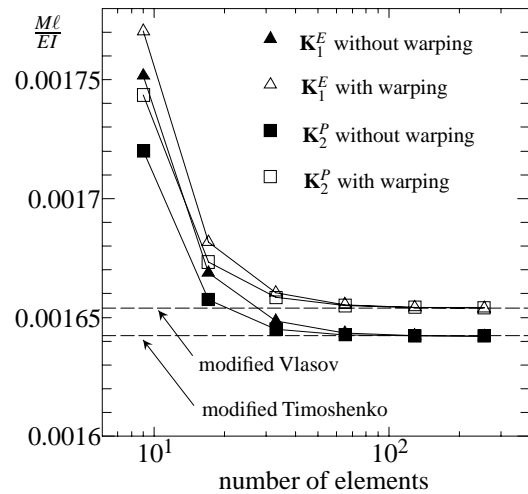
Figure 3 : Convergence to buckling solutions (a)

Euler's angles. The tangent stiffness matrix $\mathbf{K}_1$ is symmetric only in equilibrium state, while the tangent stiffness matrix $\mathbf{K}_2$ is symmetric even in non-equilibrium state, whether rotational degrees of freedom are Euler's angles or pseudo-vector components. We denote the tangent stiffness matrix derived for Euler's angles by a superscript ^{E} and denote the tangent stiffness matrix derived for rotational pseudo-vector components by ^{P} (for example: $\mathbf{K}_1^E$ is $\mathbf{K}_1$, whose rotational degrees of freedom are described by Euler's angles).

3 Numerical examples for beams

3.1 Buckling of beams under bending

Firstly we search the lateral torsional buckling problem of a circular arch under uniform bending (see Fig. (2)-a) by $\mathbf{K}_1^E$ and by $\mathbf{K}_2^P$ to compare their accuracies. Properties of the arch are; length of the arc $\ell = 10.244$ m; cross-sectional area $A = 9.288 \times 10^{-2}$ m^2; moment of inertia about the minor axis $I_y = 3.871 \times 10^{-5}$m^4;

moment of inertia about the major axis $I_x = 1.163 \times 10^{-4} \text{m}^4$; St. Venant's torsional constant $J = 5.89 \times 10^{-7}$ m^4; warping section constant $I_\omega = 5.5869 \times 10^{-7}$ m^6; Young's modulus $E = 200$ GPa; and shear modulus $G = 77.2$ GPa. In Fig. (3) we show the calculated non-dimensionalized moments against number of the elements for the case in which we considered warping introducing λ into degrees of freedom and for the case in which we neglect warping using only six degrees of freedom for a node. For both $\mathbf{K}_1^E$ and $\mathbf{K}_2^P$, the results with warping converge to the modified Vlasov solution [Vacharajittiphan, Woolcock and Trahair (1974)] in which influences of warping and pre-buckling in-plane displacements are considered, while the results without warping converge to the modified Timoshenko solution in which influence of only pre-buckling in-plane displacements is considered. The results by $\mathbf{K}_2^P$ converge to the analytic solutions at a little smaller number of elements than $\mathbf{K}_1^E$.

Secondly we search lateral torsional buckling of a cantilever right-angled beam subjected to a shearing force at the tip as shown in Fig. (2)-b. Properties of the beam are as follows: length of each side of the angled beam is 0.24 m; Young's modulus $E = 71.24$ GPa and shear modulus $G = 27.19$ GPa. In Fig. (4) we show the results by $\mathbf{K}_1^E$ along with the results by Simo and Vu-Quoc (1986) and Crisfield (1990) for the case in which we neglected warping. The present results agree better with the results by Crisfield (1990) than those by Simo and Vu-Quoc (1986), which have a little higher values.

Lastly we search the same right-angled beam for the case, in which we consider warping for I-section shown in Fig. (5). The results with warping have a little higher values than those without warping.

3.2 Buckling of beams under torsion

We search post-buckling behavior of a straight beam lying along z-axis subjected to a tip torsional moment as shown in Fig. (6). At the fixed end all displacements are restrained and at the other loaded end the axial translation w and the torsion θ_z are free. Assuming symmetry mode deformation, we analyze half of the beam, at whose symmetry edge (center of the original beam) u and θ_x are restrained so that the edge moves along y-axis.
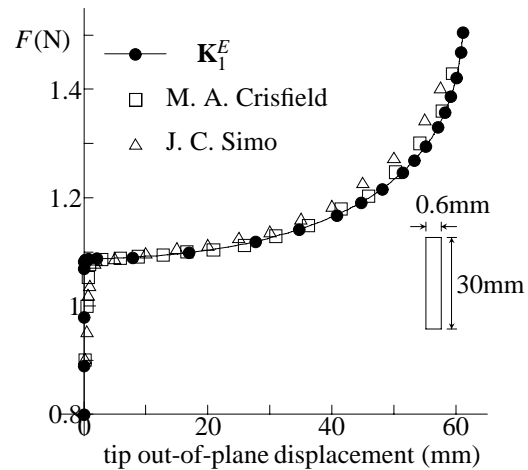
Figure 4 : Post-buckling behavior of Model (b)
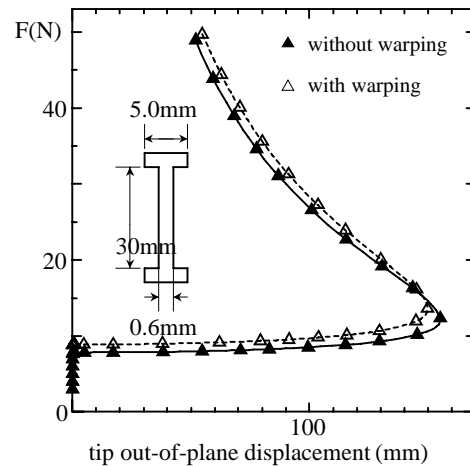
Figure 5 : Post-buckling behavior of Model (b)
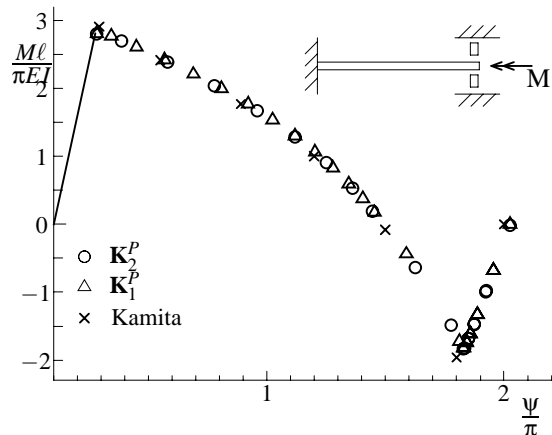
Figure 6 : Post-buckling behavior of beam under torsion
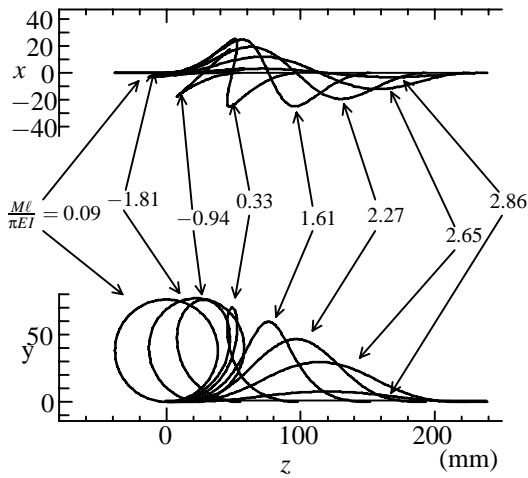
Figure 7 : Post-buckling deformation of the beam
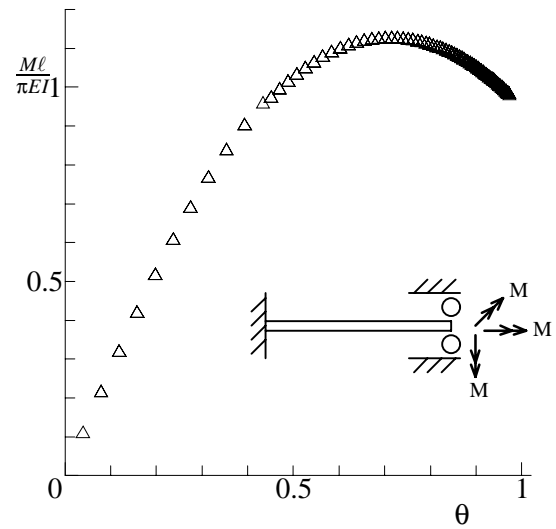
Figure 8 : Beam subjected to 3 tip moments

Properties of the beam are; Young's modulus $E = 71.24$ GPa; shear modulus $G = 27.19$ GPa; the beam length $\ell = 240$ mm; moments of inertia $I_x = I_y = 0.0833$ mm^4; and St. Venant's torsional constant $J = 2.16$ mm^4. In the calculation 60 elements are used. Relation between the torsional moment and the torsional angle is shown in Fig. (6) and the post-buckling deformation is shown in Fig. (7). The results by $\mathbf{K}_1^P$ and $\mathbf{K}_2^P$ agree better with the results by Kamita and Kondo (1995). After the first bifurcation the equilibrium path becomes instable and the torsional moment is decreasing. The perfect circular arc appears, when the torsional moment becomes 0 after the second bifurcation.

Since moment components in $\Delta\mathbf{f}$ in Eq.18 are defined as moments about spacially fixed x, y, z-axes, we secondly try to compute a beam subjected to three moments about the x, y, z-axes at the tip end as shown in Fig. (8). At the fixed end all displacements are restrained and at the other loaded tip end only two translational displacements in the directions of x, y-axes are restrained. The three applied moments have same magnitudes at the same time and are applied always about the same spacially fixed axes, while the beam axis is rotating. Properties of the beam are; Young's modulus $E = 71.24$ GPa; shear modulus $G = 27.19$ GPa; beam length $\ell = 100$ mm; moments of inertia $I_x = I_y = 0.0833$ mm^4; St. Venant's torsional constant $J = 2.16$ mm^4. In the calculation 60 elements are used for $\mathbf{K}_1^P$. Relation between magnitude of the moments and the tip principal angle (norm of the rotational pseudo-vector) is shown in Fig. (8) and the

post-buckling deformation is shown in Fig. (9). On the stable path in the beginning loading, non-symmetric deflection gradually increases. On the instable path after the peak of 3-moment loading, a small kink appears at the loaded end and is growing, as the moments are unloading.

4   Extension to plate element

4.1   *Formulation for plate element*

In this section we try to extend the previously shown formulation derived for a beam element also to a plate element. We suppose a rectangular plate, whose right-angled sides are initially lying on the spacially fixed x and y-axes as shown in Fig. (10). We denote the vertices by nodes 1, 2, 3 and 4 in order of the right-hand-screw direction of z-axis so that node 1 is lying on the origin $(0, 0, 0)$, node 2 $(a, 0, 0)$ and node 3 $(a, b, 0)$. We denote the nodal displacement vector of nodes 1-4 by

$$\mathbf{d} \equiv \left\lfloor \mathbf{d}_1^T \ \mathbf{d}_2^T \ \mathbf{d}_3^T \ \mathbf{d}_4^T \right\rfloor^T \tag{20}$$

$$\mathbf{d}_i \equiv \left\lfloor u_i \ v_i \ w_i \ \alpha_i \ \gamma_i \ \phi_i \right\rfloor^T$$
$$(i = 1, 2, 3, 4)$$

where $\mathbf{d}_i$ is a displacement vector at node i; u_i, v_i and w_i are translational displacements in the directions of x, y and z-axes respectively; α_i, γ_i and ϕ_i are Euler's angles
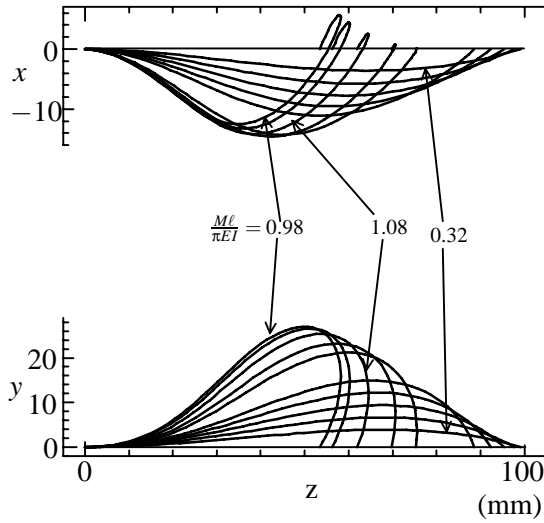
Figure 9 : Post-buckling deformation of the beam
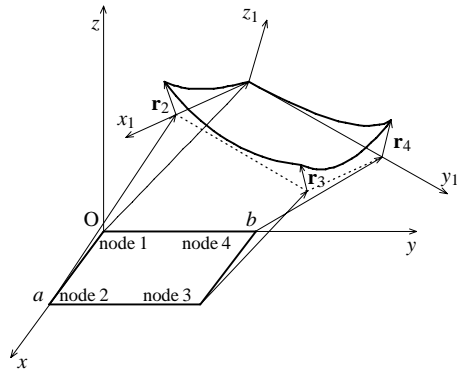
Figure 10 : Nodal relative displacements

as shown in the previous section. Using components of $\mathbf{d}_i$ we define relative displacement vectors of the nodes to node 1 in the same manner used to derive Eq.9 as follows.

$$
\mathbf{r} \equiv \lfloor \mathbf{r}_1^T \ \mathbf{r}_2^T \ \mathbf{r}_3^T \ \mathbf{r}_4^T \rfloor^T \tag{21}
$$

$$
\mathbf{r}_i \equiv \lfloor r_i^u \ r_i^v \ r_i^w \ r_i^{\theta x} \ r_i^{\theta y} \ r_i^{\theta z} \rfloor^T \tag{22}
$$

$$
= \left[\left\{ \begin{array}{c} u_i - u_1 \\ v_i - v_1 \\ w_i - w_1 \end{array} \right\} - \mathbf{T} \left\{ \begin{array}{c} \xi_i a \\ \eta_i b \\ 0 \end{array} \right\} + \left\{ \begin{array}{c} \xi_i a \\ \eta_i b \\ 0 \end{array} \right\} \right.
$$

$$
\left. \begin{bmatrix} -\cos\frac{\gamma_1+\gamma_i}{2} & 0 & \sin\frac{\gamma_1+\gamma_i}{2}\cos\frac{\alpha_1+\alpha_i}{2} \\ 0 & 1 & \sin\frac{\alpha_1+\alpha_i}{2} \\ -\sin\frac{\gamma_1+\gamma_i}{2} & 0 & \cos\frac{\gamma_1+\gamma_i}{2}\cos\frac{\alpha_1+\alpha_i}{2} \end{bmatrix} \left\{ \begin{array}{c} \alpha_i - \alpha_1 \\ \gamma_i - \gamma_1 \\ \phi_i - \phi_1 \end{array} \right\} \right]
$$

$$
(i = 1, 2, 3, 4)
$$

$$
(\xi_1, \xi_2, \xi_3, \xi_4) = (0, 1, 1, 0)
$$

$$
(\eta_1, \eta_2, \eta_3, \eta_4) = (0, 0, 1, 1)
$$

And we denote the nodal force vector of nodes 1-4 by

$$
\mathbf{f} \equiv \lfloor \mathbf{f}_1^T \ \mathbf{f}_2^T \ \mathbf{f}_3^T \ \mathbf{f}_4^T \rfloor^T \tag{23}
$$

$$
\mathbf{f}_i \equiv \lfloor F_{xi} \ F_{yi} \ F_{zi} \ M_{xi} \ M_{yi} \ M_{zi} \rfloor^T
$$

$$
(i = 1, 2, 3, 4)
$$

where F_{xi}, F_{yi} and F_{zi} are nodal forces in the directions of x, y and z-axes respectively; M_{xi}, M_{yi} and M_{zi} are nodal moments in the right-hand-screw directions of x, y and z-axes respectively. If we define the local force vector $\mathbf{f}_\ell$ and the local nodal relative displacement vector $\mathbf{r}_\ell$ operating appropriate transformation matrices for $\mathbf{f}$ and $\mathbf{d}$, we can write the stiffness equation of the plate element in the local coordinate system (x_1, y_1, z_1) as follows.

$$
\mathbf{f}_\ell = \mathbf{K}\mathbf{r}_\ell \tag{24}
$$

We decide components of $\mathbf{K}$ in Eq.24 in the following manner. As matrix components relating (F_{xi}, F_{yi}) with (r_i^u, r_i^v), we utilize components of the linear elastic stiffness matrix for the rectangular plane-stress element [Yang (1986)] and as matrix components relating (F_{zi}, M_{xi}, M_{yi}) with $(r_i^w, r_i^{\theta x}, r_i^{\theta y})$, we utilize the linear elastic stiffness matrix for the rectangular plate-bending element [Gallagher (1975)]. As matrix components relating M_{zi} with $r_i^{\theta z}$, we assume the following rigidity constants [Zienkiewcz (1977)], so that equilibrium of moments holds as

$$
\left\{ \begin{array}{c} M_{z1} \\ M_{z2} \\ M_{z3} \\ M_{z4} \end{array} \right\} = \beta E t A \begin{bmatrix} 1 & -\frac{1}{3} & -\frac{1}{3} & -\frac{1}{3} \\ -\frac{1}{3} & 1 & -\frac{1}{3} & -\frac{1}{3} \\ -\frac{1}{3} & -\frac{1}{3} & 1 & -\frac{1}{3} \\ -\frac{1}{3} & -\frac{1}{3} & -\frac{1}{3} & 1 \end{bmatrix} \left\{ \begin{array}{c} \theta_{z1} \\ \theta_{z2} \\ \theta_{z3} \\ \theta_{z4} \end{array} \right\} \tag{25}
$$

where E is Young's modulus; t is the plate thickness; A is area of the plate plane; and β is a positive constant, whose value is near 0 as far as calculation is possible. Rewriting Eq.24 into the global coordinate expression, we can derive the stiffness equation for the plate element.
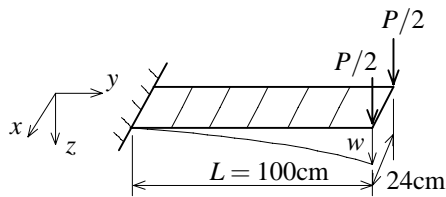
Figure 11 : Cantilever model of elastica problem
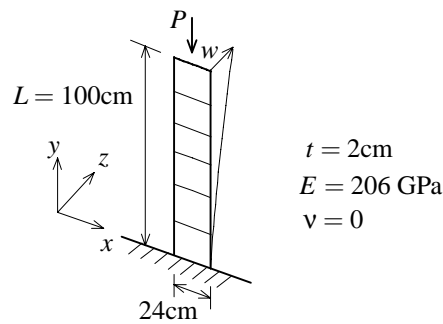
Figure 13 : Column model of elastica problem
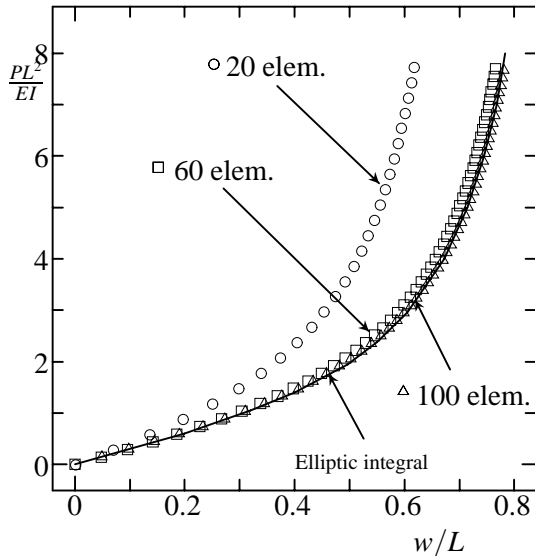
Figure 12 : Elastica curve of the cantilever
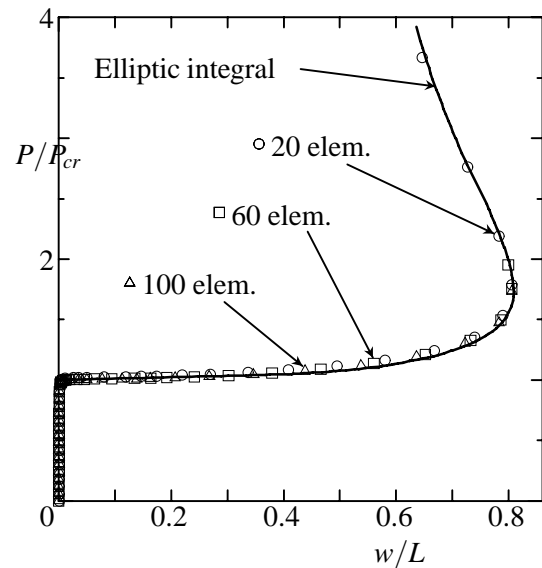
Figure 14 : Elastica curve of the column

4.2 Numerical examples for plates

Firstly we search an elastica problem of a cantilever beam modeled by plate elements as shown in Fig. (11).

One of the beam end is fixed and the other free end is subjected to two shearing forces $P/2$ at the two tip nodes as shown in Fig. (11). Properties of the beam are; Young's modulus $E = 206$ GPa; the beam length $L = 100$ cm; width of the plate element is 24 cm; thickness of the plate element is 2 cm; and Poisson's ratio is 0. We divide axial direction of the cantilever beam by elements, while we use only one element for the width direction as shown in Fig. (11). Relation between the tip deflection of the beam and the load is shown in Fig. (12) along with the solution by elliptic integral. The present results become close to the results by the elliptic integral solution, as number of the elements are increasing from 20 to 60 and in case with 100 elements the present results well agree with the results by the

elliptic integral solution. In this connection the results calculated by the beam-element formulation $\mathbf{K}_1^E$ even with 20 elements well agree with the results by the elliptic integral solution.

Secondly we search elastica problem of a column beam modeled by plate elements as shown in Fig. (13). One of the beam end is fixed and the other free end is subjected to two axial forces $P/2$ at the two tip nodes. Properties of the beam are same as the previous cantilever beam. We divide axial direction of the beam by elements, while we use only one element for the width direction as shown in Fig. (13). Relation between the tip axial displacement of the beam and the load is shown in Fig. (14) along with the solution by elliptic integral. The present results well agree with those by the elliptic integral solution even in

case with 20 elements.

Lastly we search out-of-plane buckling of a square plate as shown in Fig. (15). The plate is simply supported at four sides and subjected to uniform compressional stress σ at two parallel sides as shown in Fig. (15). Properties of the plate are; Young's modulus $E = 206$ GPa; Poisson's ratio is 0.25; thickness of the plate is 1 cm; and width of the plate is 100 cm. We analyze only 1/4 part of the plate considering the symmetry condition and divide the part uniformly in *x* and *y* directions by square elements as shown in Fig. (15). We show in Fig. (16) relation between the relative error of the present buckling stress to the analytic solution by Timoshenko and Gere (1961) and number of elements in log-log plot. Since the plots are distributed on the straight line at area with greater number of elements, the present results seem to converge to the analytic solution.

5   Summary

We formulated the tangent stiffness equation for a straight beam element whose rotational degrees of freedom are components about three axes of the right-angled Cartesian coordinate system, while the transformation matrix of the formulation is described by rotational parameters like Euler's angles. We compared numerical solutions by the formulation with those by the other formulation whose rotational degrees of freedom and transformation matrix are both described by rotational pseudo-vector components. The solutions by the both formulations converged to the same analytic solution. We calculated buckling of beams considering warping and found that the warping effect influences not only the buckling load but also the post-buckling behavior. We extended the formulation also to a rectangular plate element and confirm that the formulation using rotational degrees of freedom about the three axes can be utilized for a plate element.

References

Argyris, J(1982): Excursion into large rotations, *Comput. Meths. in Appl. Mech. and Eng.*, Vol. 32, 85-155.
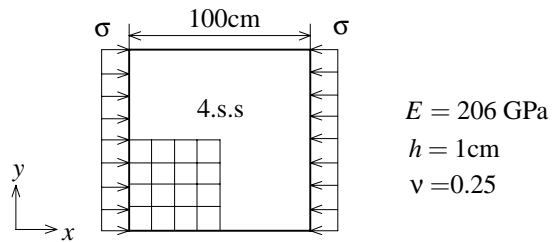
Figure 15 : Model of square plate
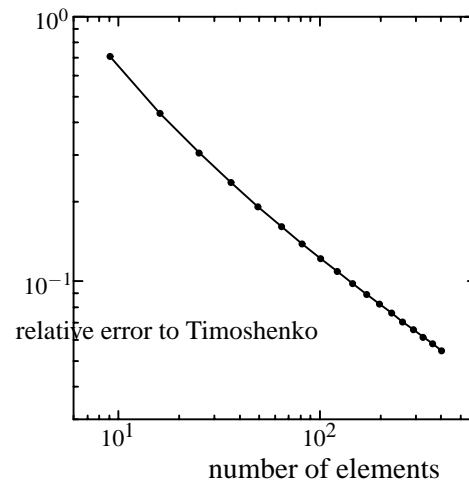
Figure 16 : Out-of-plane buckling of the square plate

Atluri, S.N.; Cazzani, A. (1995): Rotations in Computational Solid Mechanics, *Archives for Computational Methods in Engineering*, vol. 2, pp. 49-138.

Béda, P. B.(2003): On Deformation of an Euler-Bernolli Beam under Terminal Force and Couple, *CMES: Computer Modeling in Engineering & Sciences* , vol. 4, No. 2.

Cheng, H. H.; Gupta, K. C.(1989): An Historical Note on Finite Rotations, *J. of Appl. Mech.*, Vol. 56, 139-145.

Crisfield, M. A.(1990): A consistent co-rotational formulation for non-linear, three-dimensional, beam-elements, *Comput. Meths. in Appl. Mech. and Eng.*, 81, pp. 131-150.

Gallagher,R.H.(1975): Finite element analysis fundamentals, *Prentice-Hall, Inc., Englewood Cliffs, N. J.*

Goto, Y.; Morikawa, Y.; Matsuura, S.(1988): Direct lagrangian nonlinear analysis of elastic space rods using transfer matrix technique (English), *Proc. of JSCE,*

Struct. Eng./Earthquake Eng. Vol. 5, No.1, 151s-160s.

Goto,Y.; Li, X.; Kasugai, T.; Obata, M.(1995): Analysis of Greenhill problem by a co-rotational method (English), *J. of Struct. Eng. JSCE*, Vol. 41A, 411-420.

Gotou H.; Kobayasi H; Iwakuma T.(1997): A Simple Finite Displacement Formulation Using Eulerian Angles (Japanese), *J. of Struct. Eng. JSCE*, Vol. 43A, 333-338.

Gotou H.; Kobayasi H.; Saiki I.; Iwakuma T.(1998): Spacial Beam Analysis Using Degree of Rotational Freedom about 3 axes of Rectangular Cartesian Coordinates (Japanese), *J. of Appl. Mech. JSCE*, Vol. 1, 319-327.

Ishihara, M.(1996): Finite Element Formulation for 3-Dimensional Large Rotation Analysis of a Beam (Part I & II) (Japanese), *J.of Japan Society for Aeronautical and Space Sciences*, Vol. 44, 691-704.

Kamita, T. and Kondo, K.(1995): Large Displacement Finite Element Analysis of Spatial Beams (Part I & II) (Japanese), *J. of Japan Society for Aeronautical and Space Sciences*, Vol. 43, 335-349.

Okamoto, S. and Omura, Y.(2003): Finite-Element Nonlinear Dynamics of Flexible Structures in Three Dimensions, *CMES: Computer Modeling in Engineering & Sciences* , vol. 4, No. 2, pp...

Simo, J. C.; Vu-Quoc, L.(1986): A three-dimensional finite strain rod model. Part II: Computational Aspects, *Comput. Meths. in Appl. Mech. and Eng.*, Vol. 58, 79-116.

Timoshenko, S. P.; Gere, J. M.(1961): Theory of elastic stability, 3rd ed., *McGraw-Hill, New York*.

Vacharajittiphan, P.; Woolcock, S. T.; Trahair, N. S.(1974): Effect of in-plane deformation on lateral buckling, *J. Struct. Mech.*, ASCE, Vol. 3(1), 29-60.

Yang, T. Y.(1986): Finite Element Structural Analysis, *Prentice-Hall, Inc., Englewood Cliffs, N. J.*

Ziegler, H.(1982): Arguments for and against Engesser's buckling formulas, *Ing. Arch.*, Vol.52, pp.105–113.

Zienkiewcz, O. C.(1977): The finite element method, third edition, *Mcgraw-Hill, London*.